Membrane Water Treatment, *Vol. 6, No. 6 (2015) 513-524*
DOI: http://dx.doi.org/10.12989/mwt.2015.6.6.513

CFD simulations of the fluid flow behavior in a spacer-filled membrane module

Chen L. Jun [1,2], Jia Y. Xiang [*1,2] and Hu Y. Dong [1,2]

[1] *Key Laboratory of Marine Chemistry Theory and Technology, Ministry of Education, China*
[2] *College of Chemistry and Chemical Engineering, Ocean University of China, Qingdao 266100, Shandong Province, China*

(*Received November 04, 2014, Revised June 12, 2015, Accepted November 05, 2015*)

Abstract. In this study, the effects of the angles of spacer filaments and the different feed Reynolds number on the fluid flow behavior have been investigated. Three-dimensional computational fluid dynamics (CFD) study is carried out for fluid flow through rectangular channels within different angles (30°, 40°, 50°, 60°, 70°, 80°, 90°, 100°, 110°, 120°, respectively) between two filaments of spacer for membrane modules. The results show that the feed Reynolds number and the angles of spacer filaments have an important influence on pressure drop. While the feed Reynolds number is fixed, the optimal angle of spacer should be between 80° to 90°, because the pressure drop is not only relatively small, but also high flow rate region expanded significantly with the increase of the angles between 80° to 90°.The Contours of velocities and change of the average shear stress with the different angle of spacer filaments confirm the conclusion.

Keywords: computational fluid dynamics (CFD); membrane spacers; pressure drop

1. Introduction

The shortage of natural fresh water has been a serious problem for many countries in the world. A variety of desalination technologies has been developed over the years on the basis of thermal distillation, membrane separation, freezing, etc Khawaji *et al*. (2008), Delyannis and Belessiotis (2010), Pouliot (2008). Membrane-based separation applications have been rapidly gaining practical attention of the past decades Deng *et al*. (2015), Walker *et al*. (2014), Garcia-Vasquez *et al*. (2013), Strathmann (2010). However, many membrane processes are severely influenced by concentration polarization Cao *et al*. (2001), Saremirad *et al*. (2012). This phenomenon has adverse effects on the membrane performance, namely the increase of the rate of membrane fouling and the decrease of the productivity and the quality of the permeated water Sousa *et al*. (2014). Both membrane properties determine to a very large extent the usefulness of a process in a certain application. Other aspects such as the process design and spacer geometry are also of importance. The spacer lay between adjacent membranes which plays important role, one hand, keeping adjacent membrane leaves apart so as to form a feed channel, and on the other hand, increasing pressure drop and creating stagnation zones where the concentration polarization phenomena and fouling becomes weakened. The pressure drop and spatial distribution of mass

*Corresponding author, Professor, E-mail: jiayx76@aliyun.com

 ISSN: 2005-8624 (Print), 2092-7037 (Online)

transfer coefficients and hence fouling pattern on the membrane surface depend on the spacer geometric parameters such as filament spacing, thickness and flow attack angle Li and Tung (2008), Koutsou *et al*. (2007), Balster *et al*. (2010), Lipnizki and Jonsson (2002), Al-Sharif *et al*. (2013), Ahmad and Lau (2006), Li *et al*. (2004), Shakaib *et al*. (2007), Kodým *et al*. (2011), Li *et al*. (2002). It is significant that precise reveal of the hydrodynamics and concentration polarization phenomenon in the spacer-filled membrane, in order to ensure concentration polarization phenomenon can be minimized at minimum energy consumption, since the presence of feed spacer is plausible to increase pressure drop.

Flow modeling or concentration polarization on membrane surfaces that has been performed by computational fluid dynamics has proven to be a powerful tool for the study of flow patterns in membrane systems. Several experimental and theoretical studies have appeared aiming at understanding the underlying phenomena and optimizing spacer configuration. Balster *et al*. (2006) have verified and compared the performance of Standard non-woven and multi-layer net spacers in the light of mass transfer enhancement and cross-flow power consumption, respectively. The experimental results show that when the diameter of the filament of the middle spacer is reduced, the same mass transfer enhancement can be reached at 30 time lower cross-flow power consumption. And at the same cross-flow power consumption the developed multi-layer spacer shows 20% higher mass transfer than a standard commercial non-woven net spacer. Sandeep and Kumar (2001) has simulated fluid flow through rectangular channels filled with several commercially available spacers for membrane modules and compared results with literature experimental data. The results also suggest that spacers with equal filament diameters usually result in a higher pressure drop across the channel and such symmetric spacers also result in a more uniform shear rate at the top and bottom faces of the test cell, while asymmetric spacers (spacers with unequal filament diameters) resulted in lower pressure drop and also induced unequal shear rate on the top and bottom faces of the test cell. Shakaib *et al*. (2007) have studied the effect of spacer geometry on fluid dynamics and mass transfer in feed channels of spiral wound membranes. The results show that spacer geometric parameters such as filament spacing, thickness and flow attack angle have significant influence on wall shear rates and mass transfer coefficients. Ahmad and Lau (2006) have simulated three types of spacer filament geometries, which are the circular, square and triangular shape, respectively, in controlling concentration polarization and pressure drop. According to the simulation, they found that triangular filament demonstrated the highest degree of concentration minimization ability and pressure drop comparing to square and circular filaments. And the results also suggest that the usage of circular filament is recommended for energy minimization in the high feed Reynolds number.

Previous research have devoted to the effect of spacer configuration and spacer filament geometries on fluid dynamics and mass transfer. This paper mainly discusses the effects of the angle of circular spacer filaments and fluctuation of the feed Reynolds number on pressure drop through the three-dimensional simulation. Besides, in order to find out the optimal angle between space filaments, the contours of velocity and average shear stress near membrane surface are analyzed. The specific details will be discussed and explained in the following.

2. Modeling procedure and governing equations

In this paper, the length and width of the spacer are 80 mm and 32 mm, respectively. The height of the channel is 1 mm, see Fig. 1(a). In Fig. 1(b), l_t and l_b are the distances of spacer

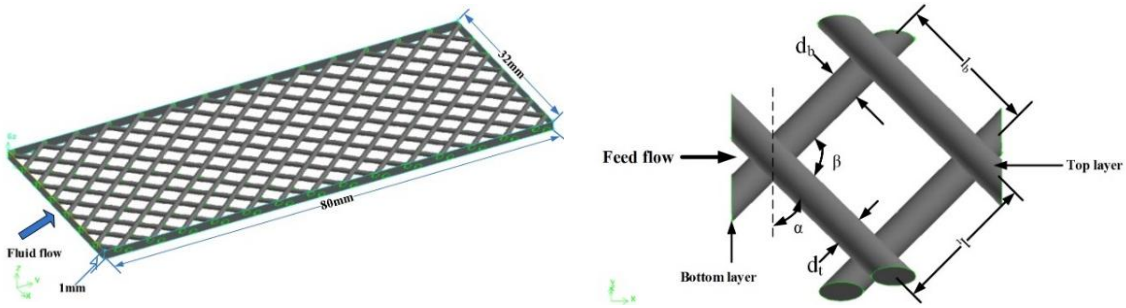

(a) The spacer in the simulation (b) The geometric characterization of a spacerd

Fig. 1 Schematics and computational domains for spacer in this paper

filaments at top and bottom layers, respectively, and they are both 3 mm. α represents the flow attack angle; β is the angle between the crossing filaments which vary from 30° to 120°. D_t denotes the top layer spacer filament diameter; d_b is the bottom layer spacer filament diameter.

The diameters of spacer filaments are set to a constant 0.5 mm, and the filaments overlap at the center of its lateral faces. Fluid flows along the *y*-axis. $Y = 0$ plane is as the velocity inlet while $Y =$ 80 plane is the outflow. The fluid is water which is assumed to be incompressible and isothermal with constant property. The feed Reynolds number is from 200 to 1800.

The Reynolds number *Re* is defined by the flow velocity u, the hydraulic diameter d_h, viscosity μ and density ρ.

$$R_e = \frac{d_h \cdot u \cdot \rho}{\mu} \tag{1}$$

Several approaches have been used to calculate the hydraulic diameter in the spacer filled channels. In this paper, the hydraulic diameter d_h is defined by

$$d_h = \frac{4 \times \text{cross} - \text{section of the flow channel}}{\text{wetted circumference}} \tag{2}$$

The governing equations for steady, laminar and three-dimensional flow are the continuity, momentum given by Eps. (1)-(4)

$$\frac{\partial u}{\partial x} + \frac{\partial v}{\partial y} + \frac{\partial w}{\partial z} = 0 \tag{3}$$

$$u\frac{\partial u}{\partial x} + v\frac{\partial u}{\partial y} + w\frac{\partial u}{\partial z} = -\frac{1}{\rho}\frac{\partial p}{\partial x} + \mu\left(\frac{\partial^2 u}{\partial x^2} + \frac{\partial^2 u}{\partial y^2} + \frac{\partial^2 u}{\partial z^2}\right) \tag{4}$$

$$u\frac{\partial v}{\partial x} + v\frac{\partial v}{\partial y} + w\frac{\partial v}{\partial z} = -\frac{1}{\rho}\frac{\partial p}{\partial y} + \mu\left(\frac{\partial^2 v}{\partial x^2} + \frac{\partial^2 v}{\partial y^2} + \frac{\partial^2 v}{\partial z^2}\right) \tag{5}$$

$$u\frac{\partial w}{\partial x} + v\frac{\partial w}{\partial y} + w\frac{\partial w}{\partial z} = -\frac{1}{\rho}\frac{\partial p}{\partial z} + \mu\left(\frac{\partial^2 w}{\partial x^2} + \frac{\partial^2 w}{\partial y^2} + \frac{\partial^2 w}{\partial z^2}\right) \tag{6}$$

In these equations, u, v, w denote the x, y, z components of the velocity, respectively; ρ is the fluid density (water, in this case); μ represents the fluid viscosity; P denotes the fluid pressure.

The y-coordinate denotes the direction of bulk flow (channel axis) with $y = 0$ corresponding to the inlet and $y = 80$ corresponding to the outlet; $z = 0$ corresponds to the bottom face of the cell and $z = h$ corresponds to the top face ($h = 1$ mm, in this case). The x-coordinate is along the width of the cell ($x = 32$ mm in this case).

The boundary conditions which describe the computational domain of the simulation are listed as follow:

Velocity inlet: $y = 0,\ u = u_y;\quad v = 0;\quad w = 0$

Outlet: $y = 80,\ p = 0$

Wall: $x = 0,\ x = 32,\ z = 0,\ z = 1,\ u = 0;\quad v = 0;\quad w = 0$

A plug flow velocity inlet was applied in the entrance of the membrane channel. Top and bottom part of the channel were treated as membrane wall. The Second Order Upwind is used for discretizing the momentum while SIMPLEC (Semi-Implicit Method for Pressure Linked Equations, Consistent) algorithm is used for pressure velocity coupling.

3. Results and discussions

Fluctuation of the feed Reynolds number (*Re*) and the angles of the spacer filaments (β) can affect effluent quality in electrodialysis equipment. These changes may cause sharp increase in pressure drop, and lead to rise in energy consumption. In order to try to identify the suitable *Re* and β, this section investigated the effects of *Re* and β on pressure drop.

CFD simulations were carried out for *Re* from 200 up to 1800, and for β from 30° up to 120°. The effects of the variation of β and *Re* were examined in detail. Fig. 2 shows the pressure drop across the test cell as a function of *Re* for all kinds of spacers (β is different just as described above).

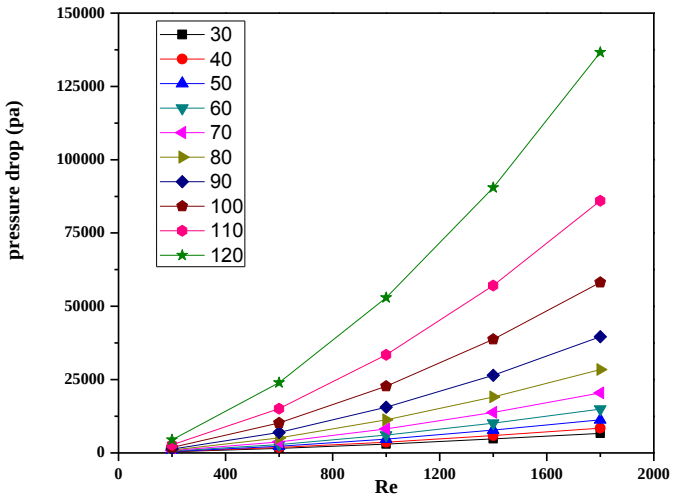

Fig. 2 Effect of *Re* on pressure drop with different angle of space filaments

Table 1 The coefficient and constant in the functional expression of pressure drop and Re

β	a	b	c	d	e
30°	0.7873×10^4	-645.1	-	-	-
40°	1.0×10^4	-941.3	-	-	-
50°	1.355×10^4	-1454	-	-	-
60°	1.792×10^4	-2027	-	-	-
70°	-	-	1.527×10^4	0.9476×10^4	-366.5
80°	-	-	2.179×10^4	1.266×10^4	-531
90°	-	-	3.09×10^4	1.715×10^4	-759.5
100°	-	-	4.597×10^4	2.457×10^4	-1117
110°	-	-	6.859×10^4	3.561×10^4	-1563
120°	-	-	1.104×10^5	5.499×10^4	-2239

As can be seen from the Fig. 2, on the whole, the pressure drop increases gradually with the increase of *Re* for the different β. Firstly, the pressure drop rises linearly with the increasing of *Re*, however the magnitude is smaller while β is at a low value, especially less than 60°. This shows the effect of *Re* on the pressure drop is smaller when β is small. The simulation results of MATLAB software indicate that pressure drop and Reynolds number satisfy the following relations when the angle is smaller than 60°

$$p = a * Re + b \tag{7}$$

Where p is pressure drop, a is the coefficient of *Re*, b is a constant, the values of a and bare listed in Table 1.

Nevertheless, there will be drastic increase in the pressure drop when β increases to 70°. The curve of pressure drop-*Re* is accord to a parabola. The relationship between them is as follows

$$P = c * Re^2 + d * Re + e \tag{8}$$

Where *p* is pressure drop, and the coefficient *c*, *d*, *e* are listed in Table 1, respectively.

From Fig. 2 and Table 1 in the above, *Re* has a significant impact on pressure drop, especially while *Re* is more than 1000. The cause could be that the fluid channel in the spacer is narrow, especially coupled with the spacer filaments. When fluid passes through the channel at a high Re, energy consumption will be very serious with the increase of pressure drop.

The spacer filaments strengthen fluid turbulence in the spacer-filled channel, so as to accelerate mass transfer effectively through reducing the concentration boundary layer. From Fig. 2, there is no question that the angles of the spacer filaments have an important influence on pressure drop. Therefore, the effect of angle of filaments (β) on pressure drop was investigated in this paper.

Fig. 3 shows pressure drop is a function of β when *Re* is constant. From Fig. 3, the change of β has a little influence to the pressure drop at a low Reynolds number (*Re* = 200, in the case). Pressure drop increases exponentially with increase of β when *Re* increase gradually. The relationship between pressure drop and β was fitted, and the relationship is as follows

$$P = \lambda * e^{kx} \tag{9}$$

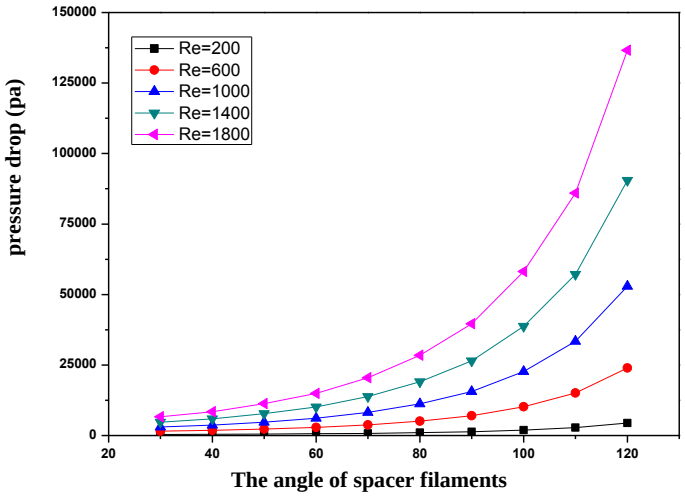

Fig. 3 Effect of the angle of space filaments on pressure drop with the different Re

Where x represents β, P represents pressure drop. The coefficient λ and k are listed in Fig. 2.

From Figs. 2 and 3, the change of β will also affect pressure drop, in particular, pressure drop rise sharply while β is larger than 80°. The reason may be that the direction of fluid flow gradually changes into perpendicular to spacer filaments, which lead to increasing of frictional resistance of fluid flow.

The above studies indicate that pressure drop rise with the increase *Re* and β. To understand the overall fluid flow in the channel and verify the above conclusion, the following investigates velocity contours in spacer channel with the different β when *Re* is fixed. The β is 30°, 40°, 50°, 60°, 70°, 80°, 90°, 100°, 110° and 120°, respectively, while *Re* is set to 1000 in this section. A z-plane (z = 0.5) is created in the middle of the channel, in detail from practical point of view. The contours plots of the velocities in z-plane for all kinds of angles are shown in Fig. 4. Primarily, it is observed that the lower regions of flow rate appear after the fluid flow pass through the intersection of filaments, just as ① and ② in Fig. 4. And then, there appears the high velocity regions in local area (③ and ④ in Fig. 4) before it reaches the next filament. The higher velocities expand significantly in the flow direction while β is larger than 80° and the turbulence of fluid also become more intense. It also can be seen that the bulk fluid velocity increases with the increase of β. The turbulence of fluid is conducive to enhancing mass transfer, and also helps to reduce fouling and decreases the boundary layer thickness.

Table 2 The coefficients in the functional expression of pressure drop and β

Re	λ	k
200	56.38	0.03605
600	237	0.03822
1000	505.6	0.03854
1400	827.5	0.03891
1800	1185	0.03936

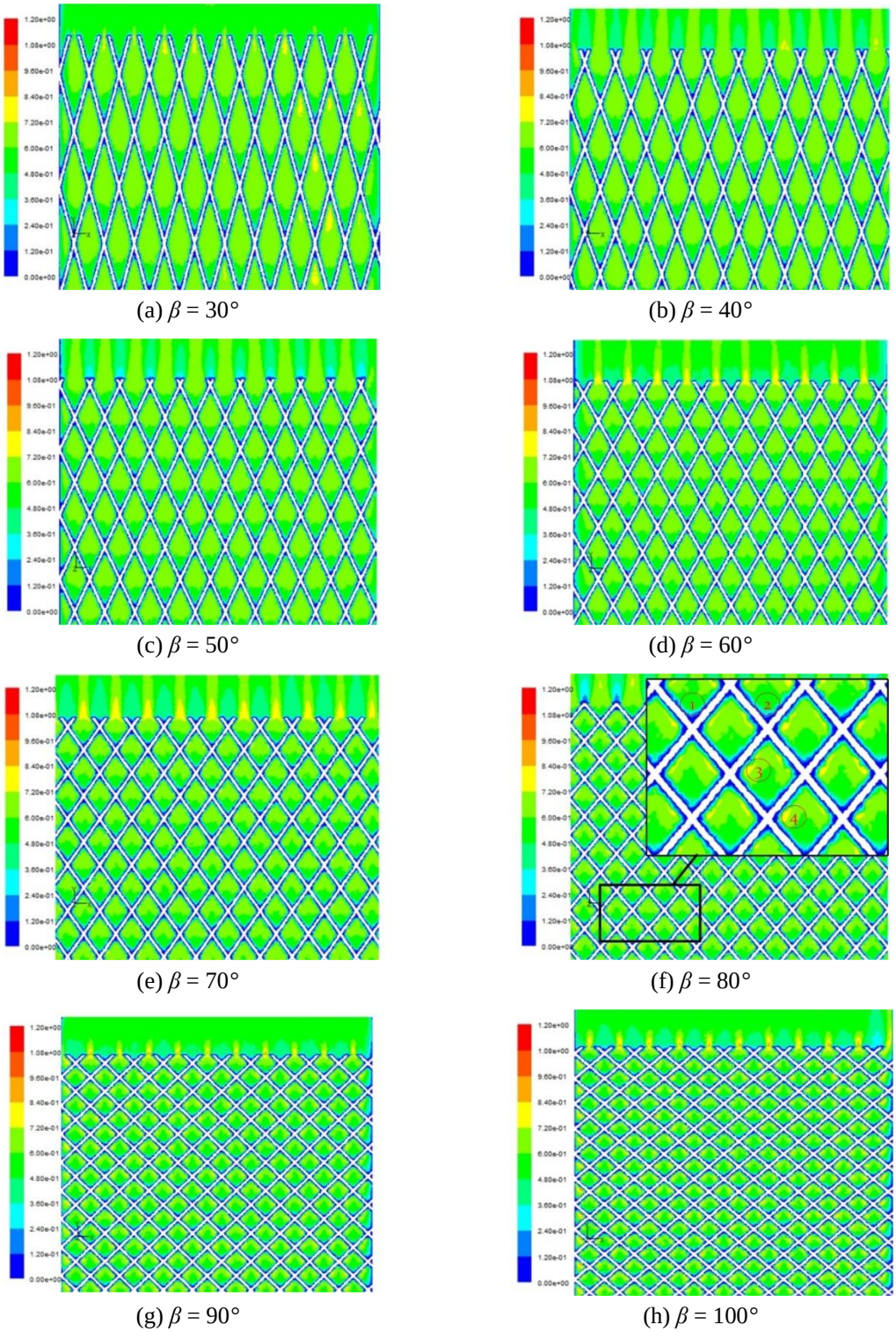

(a) β = 30° (b) β = 40°

(c) β = 50° (d) β = 60°

(e) β = 70° (f) β = 80°

(g) β = 90° (h) β = 100°

Fig. 4 Contours plots of velocities in *z*-plane (z = 0.5) for the different β

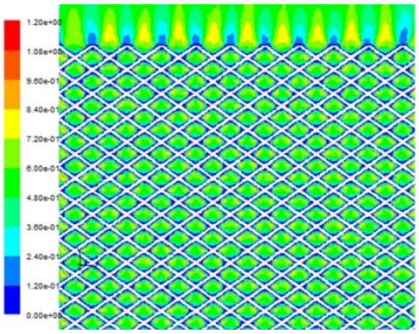

(i) β = 110°

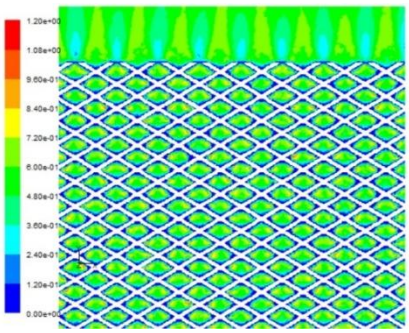

(j) β = 120°

Fig. 4 Continued

In order to understand the effect of β on velocity distribution more accurately, this paper intercept the plane X = 15 parallel to fluid flow direction and analysis the distribution of velocity on the surface. While *Re* is1000, the velocity distribution of the spacers is shown in Fig. 5. First of all, it can be seen that the maximum velocity is always larger than the initial velocity when β is changed from 30° to 120°. The maximum value increases with the increase of β. The velocity of

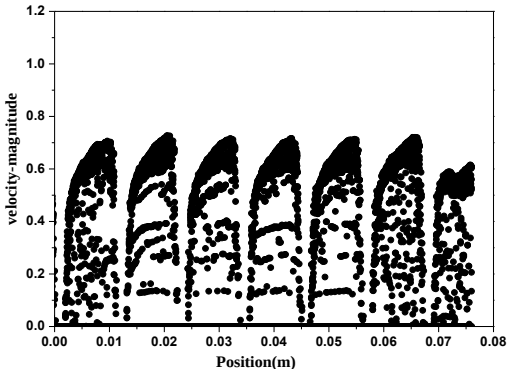

(a) β = 30°

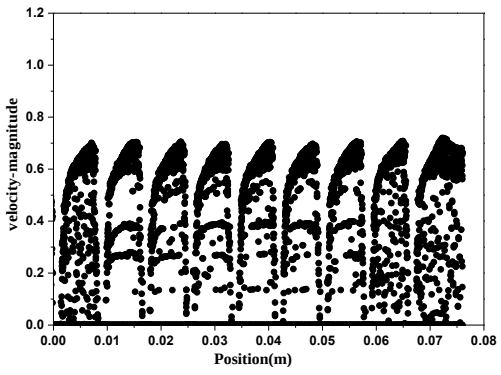

(b) β = 40°

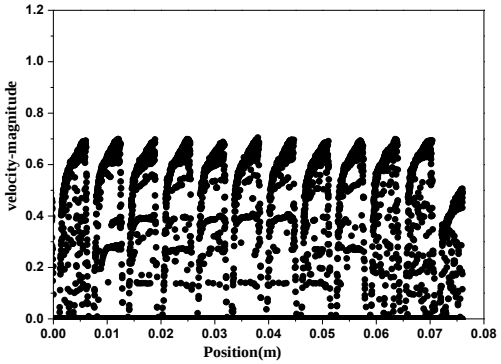

(c) β = 50°

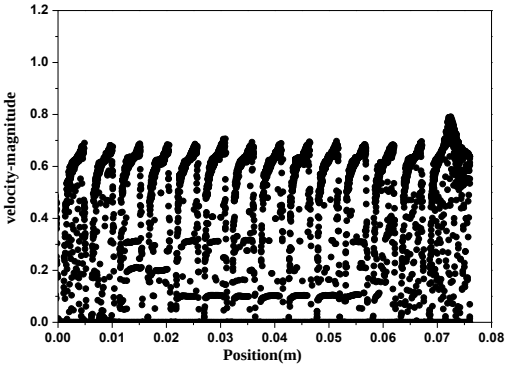

(d) β = 60°

Fig. 5 Velocity distribution at the X = 15 plane

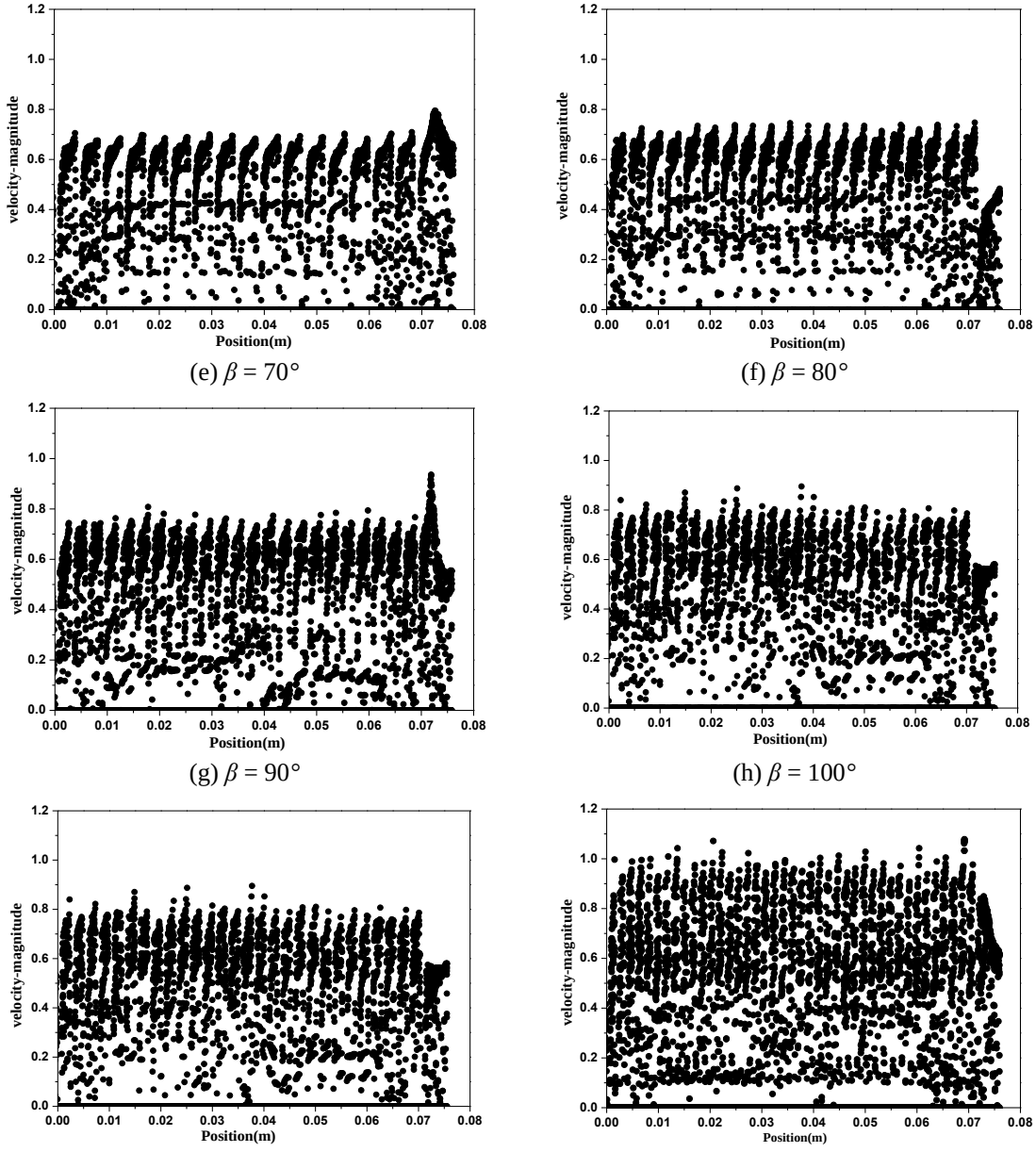

Fig. 5 Velocity distribution at the X = 15 plane

the fluid increases gradually after the fluid strikes the spacer filaments, and it achieves the maximum value before it reaches the next filament. The fluid continues to circulate periodically like this way. The higher velocities expand gradually in the flow direction with the increase of β. When β increases to 120°, the velocity of the fluid tends to be evenly distributed. Therefore we can conclude that the fluid flow will be more intense with increasing of β.

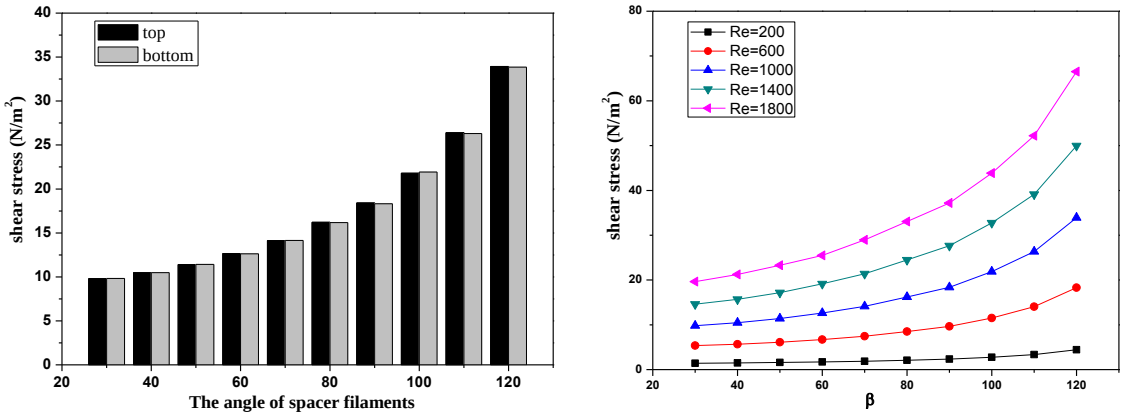

(a) (b)

Fig. 6 (a) Effect of the angle of spacer filaments on the average shear stress on the top and bottom surface; (b) Effect of the angle of spacer filaments on the average shear stress with the different *Re*

From the above, the existence of the spacer filaments causes the increasing of pressure drop in fluid channel, thus leads to the increasing of the energy consumption. However, the spacer filaments also accelerate the fluid turbulence and prevent generation of the boundary layer effectively at the same time.

Fig. 6(a) shows the average shear stress at top and bottom surface of the channel with the different β while *Re* is fixed at 1000, and Fig. 6(b) shows the average shear stress at the top surface with the different *Re*. From Fig. 6(a), it is clearly that the distributions of the average shear stress are so close at top and bottom surface of the channel, this is possible that filaments is just positioned in the middle of top and bottom membrane surface. In addition, the effect of β on the average shear stress increases with increasing of β. It can be seen that the value of the average shear stress increases from 10 to 17 when the change of β is from 30° to 80°, however the value increase from 17 to 35 when the change of β is from 80° to 120°. This is possible that there is more number of spacer filaments per meter. So the pressure drop also increases with the increasing of the average shear stress (Fig. 3). From Fig. 6(b), at lower *Re*, there is not much variation in the average shear stress for the spacer with the different β (e.g., *Re* = 200). Shear stress on the membrane surface would reduce the thickness of a concentration boundary layer and improve the mass transfer of solute at the membrane surface (Cao *et al*. 2001). This indicates that spacers with larger β can be more beneficial than the spacers with smaller β as comparable mass transfer rates can be expected, so the space with large β should be chosen to produce higher shear stress. However, from the Figs. 2 and 3, it is clearly that pressure drop increase continuously as β is increased, and increasing pressure drop could exacerbate energy consumption, thus, it prefers to use spacers with smaller β in reality. In this paper, while *Re* is relatively large, the optimal angle of spacer should be between 80° to 90° because the pressure drop couldn't be too high and the shear stress must be as large as possible.

4. Conclusions

Computational fluid dynamics simulations are carried out to investigate the effects of the angles of spacer filaments and different feed Reynolds number on the fluid flow behavior in this study.

- The feed Reynolds number has great influence on pressure drop, especially at a high Reynolds number, pressure drop grows exponentially as the feed Reynolds number increases.
- Pressure drop increases with the increase of the angle of spacer filaments. The change of the angle of spacer filaments leads to transformation of fluid behavior in the feed channel. These conclusions are confirmed by the contours plots of velocities and the change of average shear stress with the angle of spacer filaments.
- While the feed Reynolds number is relatively large, the optimal angle of sp**a**cer should be between 80° to 90° because the pressure drop couldn't be too high and the shear stress must be as large as possible.

Acknowledgments

The research described in this paper was financially supported by the Natural Science Foundation of China (21276245 and 21576249) and Key Research and Development Program of Shan-dong Province (No. 2015 GSF 117018).

References

Ahmad, A.L. and Lau, K.K. (2006), "Impact of different spacer filaments geometries on 2D unsteady hydrodynamics and concentration polarization in spiral wound membrane channel", *J. Membr. Sci.*, **286**(1-2), 77-92.

Ahmad, A.L., Lau, K.K. and Abu Bakar, M.Z. (2005), "Impact of different spacer filament geometries on concentration polarization control in narrow membrane channel", *J. Membr. Sci.*, **262**(1-2), 138-152.

Al-Sharif, S., Albeirutty, M., Cipollina, A. and Micale, G. (2013), "Modeling flow and heat transfer in spacer-filled membrane distillation channels using open source CFD code", *Desalination*, **311**, 103-112.

Balster, J., Pünt, I., Stamatialis, D.F. and Wessling, M. (2006), "Multi-layer spacer geometries with improved mass transport", *J. Membr. Sci.*, **282**(1-2), 351-361.

Balster, J., Stamatialis, D.F. and Wesslinga, M. (2010), "Membrane with integrated spacer", J. Membr. Sci., **360**(1-2), 185-189.

Cao, Z., Wiley, D.E. and Fane, A.G. (2001), "CFD simulations of net-type turbulence promoters in a narrow channel", *J. Membr. Sci.*, **185**(2), 157-176.

Delyannis, E. and Belessiotis, V. (2010), "Desalination: The recent development path", *Desalination*, **264**(3), 206-213.

Deng, D., Aouad, W., Braff, W.A., Schlumpberger, S., Suss, M.E. and Bazant, M.Z. (2015), "Water purification by shock electrodialysis: Deionization, filtration, separation, and disinfection", *Desalination*, **357**, 77-83.

Dhananjay, D., Sandeep, K.K. and Kumar, A. (2005), "Flow visualization through spacer filled channels by computationalfluid dynamics-II: improved feed spacer designs", *J. Membr. Sci.*, **249**(1-2), 41-49.

Garcia-Vasquez, W., Dammak, L., Larchet, C., Nikonenko, V., Pismenskaya, N. and Grande, D. (2013), "Evolution of anion-exchange membrane properties in a full scale electrodialysis stack", *J. Membr. Sci.*,**446**(1), 255-265.

Khawaji, A.D., Kutubkhanah, I.K. and Wie, J.M. (2008), "Advances in seawater desalination technologies", *Desalination*, **221**(1), 47-69.

Kodým, R., Vlasák, F., Šnita, D., Černin, A. and Bouzek, K. (2011), "Spatially two-dimensional mathematical model of the flow hydrodynamics in a channel filled with a net-like spacer", *J. Membr. Sci.*, **368**(1-2), 171-183.

Koutsou, C.P., Yiantsios, S.G. and Karabelas, A.J. (2007), "Direct numerical simulation of flow in spacer-filled channels: Effect of spacer geometrical characteristics", *J. Membr. Sci.*, **291**(1-2), 53-69.

Li, Y.L. and Tung, K.L. (2008), "CFD simulation of fluid flow through spacer-filled membrane module: selecting suitable cell types for periodic boundary conditions", *Desalination*, **233**(1-3), 351-358.

Li, F., Meindersma, W., de Haan, A.B. and Reith, T. (2002), "Optimization of commercial net spacers in spiral wound membrane modules", *J. Membr. Sci.*, **208**(1-2), 289-302.

Li, F., Meindersma, W., de Haan, A.B. and Reith, T. (2004), "Experimental validation of CFD mass transfer simulations in flat channels with non-woven net spacers", *J. Membr. Sci.*, **232**(1-2), 19-30.

Lipnizki, J. and Jonsson, G. (2002), "Flow dynamics and concentration polarisation in spacer-filled channels", *Desalination*, **146**(1-3), 213-217.

Pouliot, Y. (2008), "Membrane processes in dairy technology—From a simple idea to worldwide panacea", *Int. Dairy J.*, **18**(7), 735-740.

Sandeep, K.K. and Kumar, A. (2001), "Flow visualization through spacer filled channels by computational fluid dynamics I. Pressure drop and shear rate calculations for flat sheet geometry", *J. Membr. Sci.*, **193**(1), 69-84.

Saremirad, P., Gomaa, H.G. and Zhu, J. (2012), "Effect of flow oscillations on mass transfer in electrodialysis with bipolar membrane", *J. Membr. Sci.*, **405**(1), 158-166.

Shakaib, M., Hasani, S.M.F. and Mahmood, M. (2007), "Study on the effects of spacer geometry in membrane feed channels using three-dimensional computational flow modeling", *J. Membr. Sci.*, **297**(1-2), 74-89.

Shakaib, M., Hasani, S.M.F. and Mahmood, M. (2009), "CFD modeling for flow and mass transfer in spacer-obstructed membrane feed channels", *J. Membr. Sci.*, **326**(2), 270-284.

Sousa, P., Soares, A., Monteiro, E. and Rouboa, A. (2014), "A CFD study of the hydrodynamics in a desalination membrane filled with spacers", *Desalination*, **349**, 22-30.

Strathmann, H. (2010), "Electrodialysis, a mature technology with a multitude of new applications", *Desalination*, **264**(3), 268-288.

Walker, W.S., Kim, Y. and Lawler, D.F. (2014), "Treatment of model inland brackish groundwater reverse osmosis concentrate with electrodialysis—Part I: Sensitivity to superficial velocity", *Desalination*, **344**, 152-162.

RJ